molecular pharmaceutics

articles

Pharmacokinetic and Biodistribution Studies of a Bone-Targeting Drug Delivery System Based on *N*-(2-Hydroxypropyl)methacrylamide Copolymers

Dong Wang,[†,‡] Monika Sima,[†] R. Lee Mosley,[§] Jasmine P. Davda,[‡] Nicole Tietze,[†,||] Scott C. Miller,[⊥] Peter R. Gwilt,[‡] Pavla Kopečková,[†] and Jindřich Kopeček*[,†,#]

Departments of Pharmaceutics and Pharmaceutical Chemistry/CCCD and Bioengineering and Division of Radiobiology, University of Utah, Salt Lake City, Utah 84112, Department of Pharmaceutical Sciences, College of Pharmacy, and Department of Pharmacology and Experimental Neuroscience, University of Nebraska Medical Center, Omaha, Nebraska 68198

Received May 8, 2006

Abstract: Osteotropicity of novel bone-targeted HPMA copolymer conjugates has been demonstrated previously with bone histomorphometric analysis. The pharmacokinetics and biodistribution of this delivery system were investigated in the current study with healthy young *BALB/c* mice. The ^{125}I-labeled bone-targeted and control (nontargeted) HPMA copolymers were administered intravenously to mice, and their distribution to different organs and tissues was followed using a γ counter and single photon emission computed tomography (SPECT). Both the invasive and noninvasive data further confirmed that the incorporation of D-aspartic acid octapeptide (D-Asp$_8$) as bone-targeting moiety could favorably deposit the HPMA copolymers to the entire skeleton, especially to the high bone turnover sites. To evaluate the influence of molecular weight, three fractions (M_w of 24, 46, and 96 kDa) of HPMA copolymer−D-Asp$_8$ conjugate were prepared and evaluated. Higher molecular weight of the conjugate enhanced the deposition to bone due to the prolonged half-life in circulation, but it weakened the bone selectivity. A higher content of bone-targeting moiety (D-Asp$_8$) in the conjugate is desirable to achieve superior hard tissue selectivity. Further validation of the bone-targeting efficacy of the conjugates in animal models of osteoporosis and other skeletal diseases is needed in the future.

Keywords: Bone targeting; drug delivery; HPMA copolymer; SPECT; pharmacokinetics; biodistribution

Introduction

The worldwide increase of human life span is accompanied by a heavy socioeconomic burden of widespread musculoskeletal diseases and their substantial morbidity and mortality. Currently, 44 million Americans, or 55% of the people 50 years of age and older, are in danger of having

* Corresponding author: Jindřich Kopeček, Department of Pharmaceutics and Pharmaceutical Chemistry, University of Utah, 30 S. 2000 E. Rm. 201, Salt Lake City, UT 84112-5820. Phone: (801) 581-7211. Fax: (801) 581-7848. E-mail: Jindrich.Kopecek@utah.edu.

† Department of Pharmaceutics and Pharmaceutical Chemistry/CCCD, University of Utah.

‡ Department of Pharmaceutical Sciences, College of Pharmacy, University of Nebraska Medical Center.

§ Department of Pharmacology and Experimental Neuroscience, University of Nebraska Medical Center.

|| Current address: Pharmaceutical Biology-Biotechnology, Department of Pharmacy, Butenandtst. 5-13, Munich, Germany.

⊥ Division of Radiobiology, University of Utah.

Department of Bioengineering, University of Utah.

(1) Burckhardt, P.; Christiansen, C.; Fleisch, H. A. Consensus Development Conference: Prophylaxis and Treatment of Osteoporosis. *Am. J. Med.* **1991**, *90*, 107−110.

(2) *America's Bone Health: The State of Osteoporosis and Low Bone Mass in Our Nation*; National Osteoporosis Foundation: Washington, DC, 2002; pp 1−16.

(3) O'Dell, J. R. Therapeutic strategies for rheumatoid arthritis. *N. Engl. J. Med.* **2004**, *350*, 2591−2602.

(4) Firestein, G. S. Etiology and Pathogenesis of Rheumatoid Arthritis. In *Kelley's Textbook of Rheumatology*, 7th ed.; Harris, E. D., Jr., Budd, R. C., Genovese, M. C., Firestein, G. S., Sargent, J. S., Sledge, C. B., Eds.; Elsevier Saunders: Philadelphia, 2005; p 996.

(5) Wieland, H. A.; Michaelis, M.; Kirschbaum, B. J.; Rudolphi, K. A. Osteoarthritis—an untreatable disease? *Nat. Rev. Drug Discovery* **2005**, *4*, 331−344.

10.1021/mp0600539 CCC: $33.50
Published on Web 08/12/2006

osteoporosis; 10 million individuals probably already have the disease.[1,2] Similarly, arthritis, such as rheumatoid arthritis and osteoarthritis, which is always accompanied by skeletal complications, also affect tens of millions of American lives.[3−5]

However, the advancement of biomedical research in the past few decades has dramatically improved our understanding of these diseases. Many molecular targets have been identified and numerous new therapeutic agents have been developed for the treatment of musculoskeletal diseases.[6] In addition, novel concepts in drug delivery technologies have also been developed in an attempt to enhance osteotropicity of drugs and to improve their pharmacokinetic profile and therapeutic efficacy.[7]

Recently, we have developed a polymeric bone-targeting drug delivery system based on *N*-(2-hydroxypropyl)methacrylamide (HPMA) copolymer.[8,9] Alendronate (a bisphosphonate) and D-aspartic acid octapeptide (D-Asp_8) have been introduced as targeting moieties, which could favorably recognize and strongly bind to biomineral (e.g., carbonated hydroxyapatite (HA) or HA in bone) surfaces. Initial in vitro evaluation supported this hypothesis; >60% of binding to artificial HA particles was observed with targeted HPMA copolymers.[8] Similar data were obtained in preliminary studies in vivo. Injection of the delivery system to young *BALB/c* mice did not show signs of any obvious adverse events. Histomorphometric analyses of the long bones (tibia and femur) isolated from the animals demonstrated very strong accumulation of the targeted HPMA copolymers at the high bone turnover sites, such as metaphyseal spongiosa, and moderate deposition at sites of slower turnover, such as endosteum and periosteum of diaphyseal shaft. In our most recent study, it was found that, by incorporating different bone-targeting moieties, the delivery system could effectively differentiate bone formation surface from resorption surface, with D-Asp_8 preferentially binding to authentic bone resorption surfaces.[10] As the first model drug tested, prostaglandin E_1 (PGE_1, bone-anabolic agent) has also been incorporated into the delivery system via a cathepsin K specific peptide linker (Gly-Pro-Nle). Effective release of intact PGE_1 from the delivery system was observed in the presence of cathepsin K (an osteoclast-specific enzyme).[9]

In the current study, we report the first systemic pharmacokinetic and biodistribution (PK/BD) study of the HPMA copolymer-based bone-targeting delivery system on healthy young *BALB/c* mice.

Experimental Section

Materials. *N*-(2-Hydroxypropyl)methacrylamide (HPMA),[11] *N*-methacryloylaminopropyl fluorescein thiourea (MA-FITC),[12] *N*-methacryloylglycylglycine (MA-Gly-Gly-OH),[13] and *N*-methacryloyltyrosineamide (MA-Tyr-NH_2)[14] were prepared as described previously. Sephadex G-25 and LH-20 resins were obtained from GE HealthCare (Piscataway, NJ). 2-Chlorotrityl chloride resin (100−200 mesh), *N*-α-Fmoc-D-aspartic acid α-*tert*-butyl ester (Fmoc-D-Asp-OtBu), benzotriazol-1-yl-oxy-tris-pyrrolidino-phosphonium hexafluorophosphate (PyBOP), and 1-hydroxybenzotriazole hydrate (HOBt) were all purchased from Novabiochem (La Jolla, CA). Unless specified otherwise, all other reagents and solvents were purchased from Aldrich (Milwaukee, WI).

Characterization of the Synthetic Products. The weight average molecular weight (M_w) and number average molecular weight (M_n) of copolymers were determined by size exclusion chromatography (SEC) using the ÄKTA FPLC system (GE HealthCare) equipped with UV and RI detectors. SEC measurements were carried out on Superose 12 columns (HR 10/30) with PBS (pH = 7.3) as the eluent. The average molecular weights of the polymers were calculated using calibrations with narrow fractions of poly[*N*-(2-hydroxypropyl)methacrylamide] (PHPMA).

UV spectra of compounds were obtained on a Cary 400 Bio UV−visible spectrometer (Varian).

^{1}H NMR spectra of all synthesized compounds were recorded on a Varian Unity 500 MHz NMR spectrometer. The solvent peak was used for reference (d_6-DMSO, 2.49 ppm).

Mass spectra of all synthesized compounds were obtained using a Finnigan LCQ DECA mass spectrometer interfaced to an ESI source.

The D-Asp_8 peptide content in the copolymers was determined by amino acid analysis. The polymer conjugates were fully hydrolyzed, phthalic dicarboxaldehyde (OPA)-derivatized, and analyzed by a HPLC system. The amount of D-Asp_8 was calculated by calibration with standard D-Asp.

(6) Rodan, G. A.; Martin, T. J. Therapeutic approaches to bone diseases. *Science* **2000**, *289*, 1508−1514.
(7) Wang, D.; Miller, S. C.; Kopeček, J. Drug delivery for musculoskeletal diseases: Challenges and opportunities. *Adv. Drug Delivery Rev.* **2005**, *57*, 935−937.
(8) Wang, D.; Miller, S. C.; Sima, M.; Kopečková, P.; Kopeček, J. Synthesis and evaluation of water-soluble polymeric bone-targeted drug delivery systems. *Bioconjugate Chem.* **2003**, *14*, 853−859.
(9) Pan, H. Z.; Kopečková, P.; Wang, D.; Yang, J.; Miller, S. C.; Kopeček, J. Water-Soluble HPMA Copolymer−Prostaglandin Conjugates Containing a Cathepsin K Sensitive Spacer, *J. Drug Targeting*, in press.
(10) Wang, D.; Miller, S. C.; Sima, M.; Kopečková, P.; Kopeček, J. Development of polymeric drug delivery systems that can differentially target bone formation and resorption surfaces. *J. Bone Miner. Res.* **2005**, *20*, S413.
(11) Kopeček, J.; Bažilová, H. Poly[N-(2-hydroxypropyl)methacrylamide]. 1. Radical polymerization and copolymerization. *Eur. Polym. J.* **1973**, *9*, 7−14.
(12) Omelyanenko, V.; Kopečková, P.; Gentry, C.; Kopeček, J. Targetable HPMA copolymer-adriamycin conjugates. Recognition, internalization, and subcellular fate. *J. Controlled Release* **1998**, *53*, 25−37.
(13) Rejmanová, P.; Labský, J.; Kopeček, J. Aminolyses of monomeric and polymeric p-nitrophenyl esters of methacryloylated amino acids. *Makromol. Chem.* **1977**, *178*, 2159−2168.
(14) Duncan, R.; Cable, H. C.; Rejmanová, P.; Kopeček, J.; Lloyd, J. B. Tyrosinamide residues enhance pinocytic capture of N-(2-hydroxypropyl)methacrylamide copolymers. *Biochim. Biophys. Acta* **1984**, *799*, 1−8.

Synthesis of Peptides. *N*-Methacryloylglycylglycyl-(D-aspartic acid)$_8$ (MA-Gly-Gly-D-Asp$_8$) was synthesized by manual solid-phase peptide synthesis (SPPS) using Fmoc/tBu strategy on 2-chlorotrityl chloride resin.[15] After the attachment of the eighth D-aspartic acid residue onto the resin, MA-Gly-Gly-OH was coupled to the N-terminus of the resin-bound peptide with the similar PyBOP coupling procedure. The peptide product was cleaved from the resin with TFA and was then precipitated into ether, dialyzed, and lyophilized to obtain the final product. Its purity and structure were confirmed with MALDI-TOF mass spectrometry and amino acid analysis. Tyr-D-Asp$_8$ was also synthesized using a similar method.

Synthesis of HPMA Copolymers Containing D-Asp$_8$ and Tyr. HPMA copolymers were prepared by radical copolymerization of HPMA (100 mg, 0.7 mmol), MA-Tyr-NH$_2$ (4.2 mg, 0.015 mmol), and MA-Gly-Gly-D-Asp$_8$ (63 mg, 0.06 mmol) in water/DMSO (2:1) using 4,4′-azobis(4-cyanopentanoic acid) (ACA, 12 mg, 0.06 mmol) as the initiator. MPA (3-mercaptopropionic acid; 1 μL) was used as the chain transfer agent to control the molecular weight. The mixture was polymerized in a sealed ampule under nitrogen at 50 °C for 24 h. The polymer was purified by dialysis (MWCO 6−8 kDa) and isolated by lyophilization (147 mg, M_w = 67 kDa). The sample was fractionated on a Superose 12 column to produce narrow fractions with M_w of 24 kDa and 47 kDa. Similarly, a sample of M_w = 200 kDa was prepared; its fractionation produced a narrow fraction with M_w of 96 kDa. Control HPMA copolymers (no peptide) were synthesized following the same protocol.

The content of D-Asp$_8$ was determined by amino acid analysis, the content of Tyr by UV spectrophotometry.

The copolymers and Tyr-D-Asp$_8$ were radioiodinated (^{125}I) with a standard Chloramine-T assay[14] and purified with Sephadex G-25 columns.

Animal Studies. (1) Invasive PK/BD Study. All animal experiments were performed according to the University of Utah and University of Nebraska Medical Center IACUC approved protocols. ^{125}I-Labeled HPMA copolymers and Tyr-D-Asp$_8$ peptide (0.05−0.1 μCi) were administered to *BALB/c* mice (∼20 g, 5−6 mice/group) via tail vein injection. Animals were sacrificed at designated time points, and blood samples were withdrawn via the caudal vena cava. Major organs such as heart, lungs, kidneys, liver, spleen, and long bones (tibia and femur, ×2) were isolated, processed, and counted with a γ counter (Packard, Minaxi γ, Auto-gamma 5000 series, calibrated with Cs-137 nominally 0.25 μCi). The dose in blood was corrected according to the body weight of the animal.

(2) Single Photon Emission Computed Tomography (SPECT) Procedure. An animal SPECT (A-SPECT, Gamma Medica) was used to noninvasively investigate the distribution of the bone-targeting delivery system in vivo. ^{125}I-Labeled polymers and peptide (10−20 μCi, in 200 μL of saline) were given to mice (3/group) via tail vein injection, and planar images of 15 s exposure were acquired every 10−15 min for 2 h. Twenty-four hours after the injection, the animals were anesthetized with ketamine and xylazene and planar images were acquired with 1 min exposures. In order to obtain the tomographic images, the animals were put into a custom animal holder including fixed locations for placement of three aqueous radiolabeled fiducial markers offset in all three dimensions, stereotactic ear-bars, and bite-bar. For each subject, 64 exposures of 1 min were acquired at equiangular points around a 360° rotation. Images were reconstructed with digital image analysis software provided by the manufacturer.

Pharmacokinetic Analysis. Blood concentration−time profiles for each animal group were evaluated by compartmental analysis using WinNonlin software (version 3.2, Pharsight Corporation, Mountain View, CA). The pharmacokinetic parameters such as total clearance (CL), mean residence time (MRT), steady-state volume of distribution (Vd_{ss}), and biological half-life ($T_{1/2}$) were calculated from standard equations using WinNonlin. The area under the blood concentration−time curve (AUC) was calculated using the trapezoidal rule.

Statistical Analysis. The one-way ANOVA test was used to determine the statistical significance of the differences in the organ deposition among the different molecular weight P−D-Asp$_8$ conjugates. Student's unpaired *t* test was used to determine statistical significance of the differences in the organ deposition between unconjugated and conjugated polymers of different molecular weights at 24 h. $p < 0.05$ was considered statistically significant.

Results

Synthesis and Characterization of Conjugates. The structure of copolymers is shown in Figure 1, and the physicochemical characterization of all conjugates used in this study is summarized in Table 1. The fractionation of the copolymers was efficient; all polymer conjugates (fractions) showed narrow polydispersity (∼1.1). Consequently, the impact of sample heterogeneity on the pharmacokinetic (PK) and biodistribution (BD) parameters was minimal. The contents of D-Asp$_8$ in the fractionated conjugates, however, were slightly different in spite of using the same copolymerization feed ratio. The conjugate fraction with the lowest molecular weight contained the highest amount of D-Asp$_8$. Chemical heterogeneity of copolymers prepared by radical copolymerization to high conversions is a frequently observed phenomenon. All copolymers contained a small amount (∼2 mol %) of tyrosineamide moieties to permit radioiodination and detect their fate after intravenous administration to mice.

Biodistribution of the Bone-Targeting Moiety (Tyr-D-Asp$_8$) and of HPMA Copolymer−D-Asp$_8$ Conjugates. The results of body distribution of HPMA copolymer conjugates and controls are shown in Figure 2. P−D-Asp$_8$ (with different M_w) and the targeting moiety (Tyr-D-Asp$_8$) were all very

(15) Chan, W. C.; White, P. D. *Fmoc Solid-Phase Peptide Synthesis, A Practical Approach*; Oxford University Press: New York, 2000; pp 41−74.

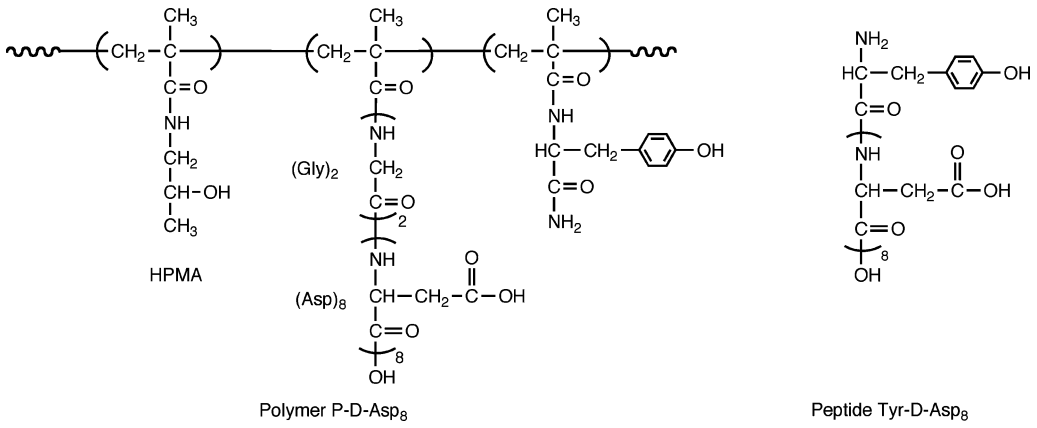

Figure 1. Structure of Tyr-labeled HPMA copolymer−D-Asp_8 conjugates and of the peptide Tyr-D-Asp_8.

Table 1. Compounds Used in the PK/BD Study

	compound	M_w (kDa)	PDI[b]	[D-Asp_8] (mol/g)	D-Asp_8 per macromolecule
1	Tyr-D-Asp_8	1.1	1.00		
2	P−D-Asp_8[a]	24	1.07	1.84×10^{-4}	4.4
3	P−D-Asp_8	46	1.07	1.21×10^{-4}	5.6
4	P−D-Asp_8	96	1.06	1.00×10^{-4}	9.6
5	$P_{control}$	23	1.03		
6	$P_{control}$	42	1.16		
7	$P_{control}$	105	1.17		

[a] P is the Tyr-labeled HPMA copolymer backbone. [b] Polydispersity (M_w/M_n).

rapidly recognized by the skeleton (represented by tibia and femur). This occurred within just 15 min following the administration of the conjugates. The deposition of D-Asp_8 and P−D-Asp_8 (25 kDa) reached maximum levels in the long bones within the first 15 min, while the accumulation of P−D-Asp_8 (46 kDa) and P−D-Asp_8 (96 kDa) increased gradually during the experimental time frame. After 24 h, the amount of P−D-Asp_8 (96 kDa) in long bones was the highest (10.76 ± 0.37% of the injected dose per gram of tissue), followed by Tyr-D-Asp_8 (4.25 ± 0.26% of the injected dose per gram of tissue) and P−D-Asp_8 (46 kDa) (3.84 ± 0.79% of the injected dose per gram of tissue); the lowest accumulation at 24 h was observed, as expected, with P−D-Asp_8 (24 kDa) (0.92 ± 0.08% of the injected dose per gram of tissue).

While the analysis of isolated tibia and femur provided representative skeleton deposition data of the conjugates, the noninvasive SPECT imaging provided a more comprehensive understanding of their distribution pattern in the whole skeleton. As shown in Figure 3, the deposition sites of the conjugates, and especially of the (free) targeting moiety in the long bones, were mainly the knee joints. On the other hand, the long bone shaft, where the bone marrow resides, only showed a weak signal of radioactivity. Other skeleton sites, such as the spine (including lumbar vertebrae), skull (including mandible and incisor roots of the rodents), and ribs were all detected with different levels of P−D-Asp_8 or Tyr-D-Asp_8 deposition. Among all the tested compounds, Tyr-D-Asp_8 demonstrated a pattern of exclusive deposition to the skeleton with minimal accumulation in the soft tissue. Tomographic imaging of the mice injected with the targeting moiety (24 h after administration, see movie 1 and movie 2 in Supporting Information) suggested that the peptide located mainly in the distal femur and proximal tibia and not in the joint cavity. For the deposition in the upper body, it was determined that the upper incisor root showed the highest deposition of the peptide, followed by lower incisor root and mandible (Figure 3).

All bone-targeting polymer conjugates tested showed different levels of distribution to soft tissues (kidneys, liver, heart, etc., Figure 2). The detected differences were statistically significant ($p < 0.05$) among all P−D-Asp_8 conjugates tested at all time points except those of 24 kDa and 46 kDa in the kidneys and bone at 1 h. The distribution of P−D-Asp_8 (24 kDa) and Tyr-D-Asp_8 to most of the organs was transient and declined to a very low level in a few hours except in kidneys. Interestingly, Tyr-D-Asp_8 (1.1 kDa) showed a slightly higher uptake in most organs (except kidneys) at the end of 24 h when compared to P−D-Asp_8 (24 kDa). The administration of higher molecular weight P−D-Asp_8 (46 kDa) demonstrated an immediate high deposition to all organs examined, with the highest injected dose per gram of tissue (6.07 ± 0.26%) found in the lung. The clearance of this polymer was slower than that of P−D-Asp_8 (24 kDa). At the end of 24 h, it showed a higher deposition in all organs when compared to P−D-Asp_8 (24 kDa) and Tyr-D-Asp_8. P−D-Asp_8-Tyr (96 kDa), the highest molecular weight bone-targeting copolymer, rapidly (within 15 min) distributed to all soft organs to very high levels, with the lungs showing the highest injected dose per gram of tissue (12.69 ± 0.55%). Although the amount of polymer deposited to the heart, lungs, and kidneys gradually decreased, the levels in liver and spleen remained almost constant at the end of 24 h. The above biodistribution data are in agreement with the SPECT imaging results (Figure 3), which show little deposition of the ^{125}I-labeled P−D-Asp_8 (24 kDa) and Tyr-D-Asp_8 in all organs at 24 h except kidneys for P−D-Asp_8 (24 kDa). Large deposition of P−D-Asp_8 (46 kDa) in the liver is clearly evident at 24 h in the SPECT images. Strong signals in bladder and urinary track are also evident for this

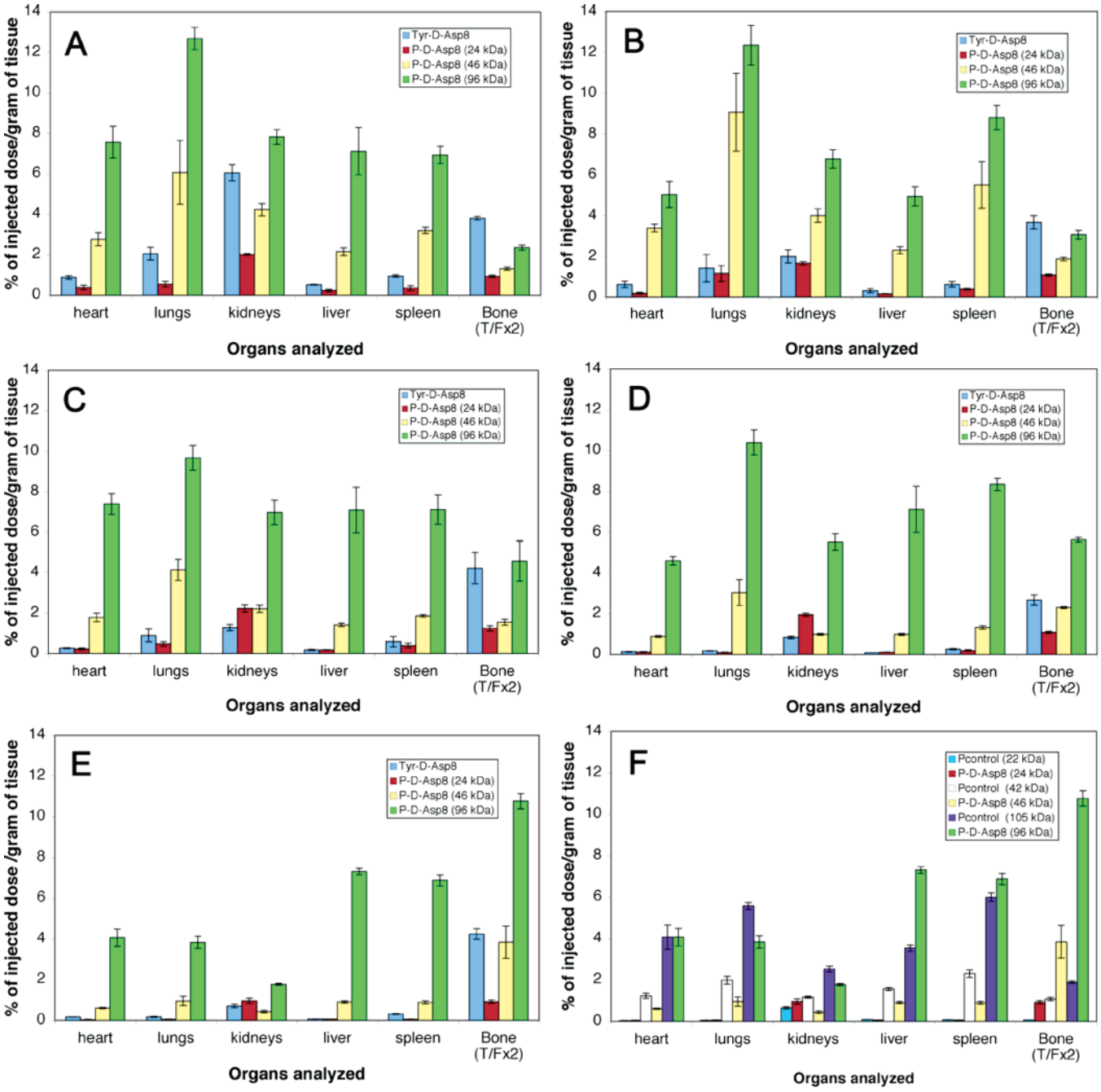

Figure 2. Effect of molecular weight on the biodistribution of Tyr-labeled HPMA copolymer−D-Asp$_8$ conjugates (P−D-Asp$_8$). HPMA copolymers (no peptide) and Tyr-D-Asp$_8$ were used as controls. The ^{125}I-labeled samples were administered intravenously to *BALB/c* mice, and the biodistribution was analyzed at the time intervals indicated: (A) 15 min, (B) 30 min, (C) 1 h, (D) 4 h, (E) 24 h. $p < 0.05$ except for P−D-Asp$_8$ (24 kDa and 46 kDa) in the kidneys and bone of panel C; (F) Twenty-four hour comparison of targeted and nontargeted conjugates. T/F×2 represents two sets of tibia and femur. The accumulation in the bone was significantly higher ($p < 0.05$) for all three P−D-Asp$_8$ as compared to their respective P$_{control}$. The targeting strategy did not result in significantly higher accumulation in any of the other organs with any of the different molecular weight conjugates except for P−D-Asp$_8$ 96 kDa, which showed a significantly higher accumulation in the liver and spleen as compared to P$_{control}$ of the similar molecular weight.

conjugate. But they may overlap with the signal from its deposition in spine. The SPECT of P−D-Asp$_8$ (96 kDa) was not performed due to the extremely high dose of the conjugate in circulation. That may result in high background, making the identification of different organs difficult.

All tested compounds showed quick distribution to the kidneys. They were significantly cleared from the kidneys by the end of 24 h except P−D-Asp$_8$-Tyr (24 kDa), which seems to be exceptionally slow in clearing from the kidneys as compared to other organs. This result was echoed by the

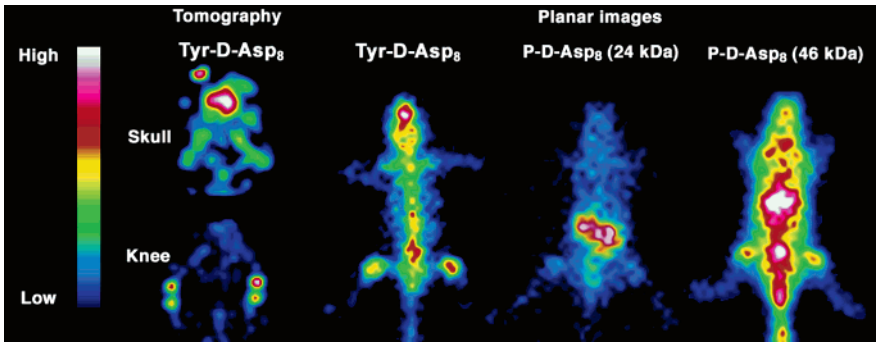

Figure 3. Planar and tomographic images of *BALB/c* mice 24 h after iv administration of Tyr-labeled HPMA copolymer−D-Asp_8 conjugates and of Tyr-D-Asp_8 recorded by single photon emission computed tomography.

SPECT imaging of the animals injected with P−D-Asp_8 (24 kDa), in which the kidney demonstrated the highest signal level (Figure 3). However, it was not possible to distinguish whether the signal was from the cortex, medulla, or pelvis of the kidneys.

For both P−D-Asp_8 conjugates (24 kDa and 46 kDa), the SPECT images (Figure 3) also indicated significant deposition in the bladder and urinary tract of some animals. However, this observation was not consistent in all animals imaged.

The distribution of control HPMA copolymers (no targeting peptide, $P_{control}$) was also evaluated at 24 h (Figure 2F). The accumulation in the bone was significantly higher ($p < 0.05$) for all three P−D-Asp_8 conjugates as compared to their respective $P_{control}$ polymers. The distribution of low molecular weight P−D-Asp_8 and $P_{control}$ (24 kDa and 22 kDa) to the soft organs was negligible except in the kidneys, where both polymers showed a deposition level of less than 1% injected dose per gram of tissue. The deposition of P−D-Asp_8 (24 kDa) to the long bones, however, was more than 10-fold higher than that of $P_{control}$ (22 kDa). For the medium sized copolymers, P−D-Asp_8 (46 kDa) demonstrated a lower deposition to all tissues tested than $P_{control}$ (42 kDa), except long bones, where P−D-Asp_8 (46 kDa) showed a more than 2-fold higher deposition than $P_{control}$ (42 kDa). For the high molecular weight copolymers tested, the bone-targeted P−D-Asp_8 (96 kDa) showed more than 4-fold higher deposition to long bones than $P_{control}$ (105 kDa). P−D-Asp_8 (96 kDa) also showed significantly higher deposition to liver and spleen than $P_{control}$ (105 kDa), while the latter showed slightly higher deposition to the lungs and kidneys. Thus, the targeting strategy did not result in higher accumulation ($p > 0.05$) in any of the soft organs with any of the different molecular weight conjugates except for P−D-Asp_8 (96 kDa) (in the liver and spleen).

Pharmacokinetic Analysis of the Tested Conjugates in Blood. The levels of the tested conjugates in the blood can be described in two groups. P−D-Asp_8 (24 kDa) and Tyr-D-Asp_8 both showed very low levels in the blood even at 15 min postadministration, with Tyr-D-Asp_8 showing a higher concentration of 2.22 ± 0.27% of the injected dose. The levels of both compounds rapidly declined to less than 0.5% of the injected dose. On the other hand, both P−D-Asp_8 (46 kDa) and P−D-Asp_8 (96 kDa) showed very high initial levels in blood (15.76 ± 0.76% and 34.87 ± 3.61% of the injected dose, respectively) followed by a gradual decline. At the end of 24 h, only 0.54 ± 0.08% of the administered P−D-Asp_8 (46 kDa) dose remained in blood while a much higher level was detected (11.10 ± 2.47%) for P−D-Asp_8 (96 kDa).

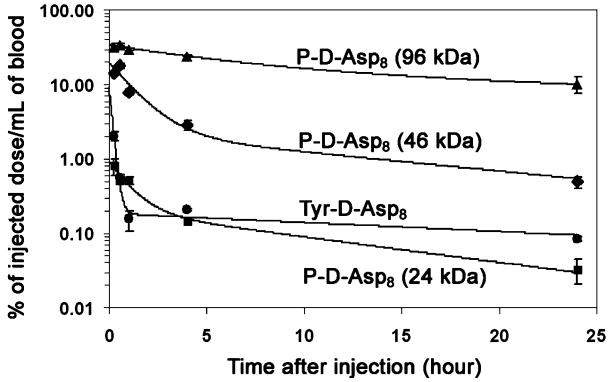

Figure 4. Blood clearance of ^{125}I-labeled HPMA copolymer−D-Asp_8 conjugates after intravenous administration to *BALB/c* mice. Radioactivity in the bloodstream (% injected dose) is shown for conjugates of different molecular weight and for Tyr-D-Asp_8.

Table 2. Pharmacokinetic Parameters for Tested Compounds with Different M_w

compound	AUC (% dose/ (mL h))	α $T_{1/2}$ (h)	β $T_{1/2}$ (h)	CL (mL/h)	MRT (h)	Vd_{ss} (mL)
Tyr-D-Asp_8	8.04	0.11	24.95	12.43	29.70	369.13
P−D-Asp_8[a] (24 kDa)	3.21	0.69	8.74	31.16	10.04	312.75
P−D-Asp_8 (46 kDa)	60.18	0.90	11.77	1.66	11.11	18.45
P−D-Asp_8 (96 kDa)	978.41	4.62	41.28	0.10	52.57	5.37

[a] P is the Tyr-labeled HPMA copolymer backbone.

Figure 4 illustrates the blood clearance of HPMA copolymer conjugates. A two-compartment model with iv bolus input best described the blood concentration−time data for all the groups. The pharmacokinetic parameters obtained for each group are summarized in Table 2. The elimination half-lives ($T_{1/2}$) of the three HPMA copolymer conjugates showed a strong correlation to molecular size, with the smallest copolymer demonstrating the shortest half-life (8.7 h). Assuming that elimination is facilitated primarily by renal

filtration, the larger molecular weight copolymers would be removed from the body at a much slower rate than the smaller ones, as reflected by the long half-life observed for the 96 kDa conjugate. Furthermore, the distribution of the 96 kDa conjugate appeared to be almost entirely restricted to the blood compartment as reflected by the low steady-state volume of distribution (Vd_{ss}). By contrast, the copolymer conjugate with the smallest molecular weight, 24 kDa, had a pronounced distribution phase, reflecting rapid initial tissue uptake. The targeting moiety Tyr-D-Asp_8 shared disposition characteristics most closely with the conjugate possessing the lowest molecular weight, P−D-Asp_8 (24 kDa), as reflected in similar pharmacokinetic parameters, i.e., relatively high clearance and volume of distribution.

Discussion

HPMA copolymer is a biocompatible water-soluble polymer that has been widely used as a drug carrier in cancer chemotherapies.[16,17] Different targeting moieties have been conjugated with HPMA copolymer to improve their tissue specificity. The incorporation of alendronate and D-Asp octapeptide into HPMA copolymers has imparted the versatile delivery system a new ability of targeting to the skeleton.[8] The histology findings are very encouraging, but the information they provide is limited. In the present PK/BD study of the bone-targeting HPMA copolymer conjugates with D-Asp_8 as targeting moiety, we designed the experiments to answer the following critical questions. (a) How efficient is the delivery system in targeting the whole skeleton? (b) What is the delivery system's subskeleton distribution pattern? (c) What is the prediction of its in vivo safety profile? (d) What can be done to further optimize the delivery system?

Both the invasive biodistribution study and the noninvasive SPECT imaging data support the effective targeting of D-Asp_8 and its copolymer conjugates to the skeleton. As can be seen in Figure 2, at the end of 24 h, the deposition of Tyr-D-Asp_8 into tibia and femur was the highest among all the organs and tissues evaluated. The SPECT imaging (Figure 3) indicated that such favorable binding was not limited to the long bones, as the peptide was also found in all the other parts of the skeleton, suggesting that Tyr-D-Asp_8 is indeed a very powerful bone-targeting moiety.

Conjugation of D-Asp_8 to HPMA copolymers imparts the bone-targeting ability to the conjugates. As shown in Figures 2 and 3, all three bone-targeting conjugates showed strong binding to the tibia and femur. Compared to nontargeted HPMA copolymers ($P_{control}$), the preference of the D-Asp_8-containing polymeric delivery systems for the skeleton was pronounced. For P−D-Asp_8 (24 kDa), the binding to bones plateaus after 15−30 min. But the accumulation of P−D-Asp_8 (46 kDa) and P−D-Asp_8 (96 kDa) increased gradually during the 24 h, with P−D-Asp_8 (96 kDa) showing the highest deposition to bone. This observation may possibly be attributed to the different half-lives of the conjugates in circulation. As shown in Table 2, the half-lives in the first phase (α $T_{1/2}$) are solely dependent on the molecular weight of the compounds. The lower the molecular weight, the faster their distribution into the organs and tissues from the blood compartment and, consequently, the shorter their half-lives. On the other hand, the half-lives for the second phase (β $T_{1/2}$) basically followed the same trend, except in the case of Tyr-D-Asp_8. Possibly, the binding of the peptide to plasma proteins may have contributed to its extended stay in blood. However, this does not seem to have an impact on Tyr-D-Asp_8 binding to bones, as it plateaus 15 min postinjection.

Apparently, the deposition of the bone-targeting delivery system to the skeleton is decided by two competing processes: (a) Distribution and binding to the bone surface and (b) elimination from the blood via kidneys. While Tyr-D-Asp_8 has the advantages of fast tissue distribution and strong bone binding, P−D-Asp_8 (96 kDa) may benefit from its long residence time in the circulation and redistribution of the bone-targeting polymer from soft tissues to the hard tissue. Indeed, P−D-Asp_8 (96 kDa) showed the highest bone accumulation 24 h post administration. However, the nonspecific accumulation of this polymer to soft tissues was also significantly higher than that of the other polymers (Figure 2E). Due to this unfavorable target-to-background ratio, the use of the very high MW polymer may not be the best option in improving the therapeutic index of the delivery system.

Among all the tested compounds, P−D-Asp_8 (24 kDa) showed the lowest deposition to the bone. Potentially, this is because it is denied of either of the advantages discussed above. The PK analysis data in Table 2 also agrees with previous findings[18] suggesting a 45 kDa glomerular filtration cutoff size for HPMA copolymers. Those with molecular weight larger than this limit would have a much longer half-life in the blood compartment.

The SPECT results revealed that the delivery system might favorably deposit all over the skeleton. Our previous histomorphometric study of long bones only provided information about deposition of the delivery system in long bones.[8,10] The current SPECT study indicated that the distribution of the HPMA copolymer-based delivery system was more favorable than initially anticipated. For Tyr-D-Asp_8, deposition was found in the knees, the spine (especially lumbar vertebrae), the ribs, and the skull. Tomographic analysis further clarified that the signals in the knees originated from the proximal tibia and distal femur. These findings agreed very well with previous histomorphometric results in which

(16) Kopeček, J. Soluble biomedical polymers. *Polim. Med.* **1977**, *7*, 191−221.

(17) Kopeček, J.; Kopečková, P.; Minko, T.; Lu, Z.-R. HPMA copolymer-anticancer drug conjugates: design, activity, and mechanism of action. *Eur. J. Pharm. Biopharm.* **2000**, *50*, 61−81.

(18) Seymour, L. W.; Duncan, R.; Strohalm, J.; Kopeček, J. Effect of molecular weight (M_w) of N-(2-hydroxypropyl)methacrylamide copolymers on body distribution and rate of excretion after subcutaneous, intraperitoneal, and intravenous administration to rats. *J. Biomed. Mater. Res.* **1987**, *21*, 1341−1358.

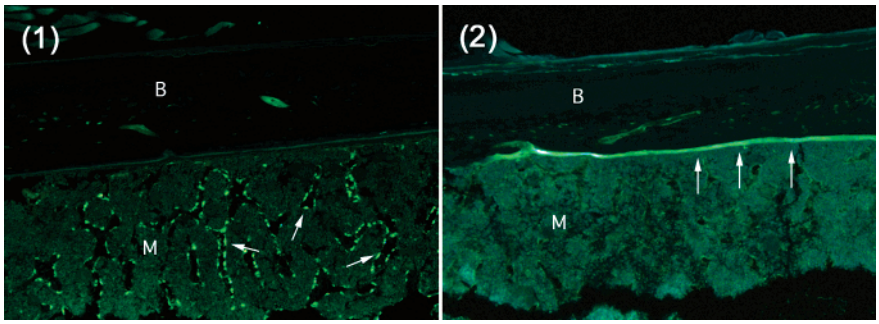

Figure 5. Histomorphometric analysis of long bones from *BALB/c* mice intravenously injected with $P_{control}$−FITC (M_w = 68 kDa, PDI = 1.5, [FITC] = 1.14 × 10^{-4} mol/g) and P−D-Asp_8-FITC (M_w = 68 kDa, PDI = 1.5, [D-Asp_8] = 1.77 × 10^{-4} mol/g, [FITC] = 1.05 × 10^{-4} mol/g). (1) Section through the mid-diaphyseal shaft illustrating the retention of the $P_{control}$−FITC in the marrow sinusoids (arrows). (2) Section through the mid-diaphyseal shaft illustrating the uptake of P−D-Asp_8-FITC on the endocortical surface (arrows). B = bone, M = marrow. Magnification 15×.

the metaphyseal spongiosa and cortex were heavily labeled but the cortical surfaces of the diaphyseal shaft were only lightly labeled.[8,10] Tomographic analysis also clarified that the signals in the skull originate from the incisor roots and mandible of the animal. From the SPECT images, it is clear that both P−D-Asp_8 (24 kDa) and P−D-Asp_8 (46 kDa) demonstrated a pattern of deposition to the skeleton similar to that of Tyr-D-Asp_8, though not as selective. These findings are of great significance because, in this animal model, all the skeletal sites mentioned above are high bone turnover sites featuring abundant blood supply. This observation suggests that this delivery system may become a very effective tool for the treatment of cancer bone metastasis, osteomyolytis, osteoarthritis, etc., which have pathological features similar to those at the high turnover sites in young healthy *BALB/c* mice. Further investigation is also needed to determine if the delivery system would provide similar targeting efficiency in models of osteoporosis and skeletal disease. The deposition pattern of the delivery system on the osteoporotic skeleton will be of particular interest.

Clearly, the targeting moiety (Tyr-D-Asp_8) possessed the best bone selectivity among all the compounds tested. Besides bone, it showed a very low level in all the other tissues and organs. The absolute deposition amount to the skeleton was also very good. Using an L-Asp_6 conjugate with estradiol, Yokogawa et al. demonstrated the therapeutic benefit of the peptide.[19] However, as the authors also noted, each peptide could only carry one drug molecule in their design. Further, the mechanism of drug release seems solely dependent on the degradation of L-Asp_6. In contrast to the peptide carrier, HPMA copolymer−D-Asp_8 conjugates could incorporate multiple drug molecules onto a single polymer chain. Various drug-releasing mechanisms (pH or specific enzyme trigger) may also be employed for optimized drug release profile.[7] However, the selectivity of HPMA copolymer−D-Asp_8 conjugates toward the hard tissue needs to be improved. P−D-Asp_8 (24 kDa) showed a relatively high deposition to kidneys, in addition to the skeleton, in agreement with results observed by Ghandehari's laboratory.[20] Potential reabsorption of the conjugate by epithelial cells of the kidneys via endocytosis may contribute to this observation.[21] However, it is not clear why P−D-Asp_8 (24 kDa) showed a higher retention than P−D-Asp_8 (46 kDa) in kidneys. For high molecular weight P−D-Asp_8 (96 kDa), its long circulating half-life enhanced its deposition to the bone. But its distribution to the well-perfused organs, especially liver and spleen, was also evident (Figures 2 and 3). The clustered negative charges from the targeting moiety may be another contributing factor to this higher deposition (compared to nontargeted HPMA copolymer), as negatively charged macromolecules may be recognized by scavenger receptors on nonparenchymal cells.[22,23] The reticuloendothelial system (RES) including macrophages, Kupffer cells of liver, reticulocytes of spleen, and bone marrow may contribute to the deposition of nontargeted HPMA copolymers to soft tissues and the bone.[21] Previous histomorphometric findings indicated that the retention sites of nontargeted HPMA copolymer in bone were seen only at the lining of marrow sinusoids, while the bone surface does not have any detectable deposition (Figure 5). Depending on the therapeutic agents to be used, the inadequate distribution of the delivery system to soft tissues may cause significant side effects in vivo. Apparently, further optimization of the HPMA copolymer−D-Asp_8 conjugates to reduce their distribution to soft tissues is necessary.

(19) Yokogawa, K.; Miya, K.; Sekido, T.; Higashi, Y.; Nomura, M.; Fujisawa, R.; Morito, K.; Masamune, Y.; Waki, Y.; Kasugai, S.; Miyamoto, K. Selective delivery of estradiol to bone by aspartic acid oligopeptide and its effects on ovariectomized mice. *Endocrinology* **2001**, *142*, 1228−1233.

(20) Mitra, A.; Nan, A.; Ghandehari, H.; McNeill, E.; Mulholland, J.; Line, B. R. Technetium-99m-Labeled N-(2-hydroxypropyl)-methacrylamide copolymers: Synthesis, characterization, and in vivo biodistribution. *Pharm. Res.* **2004**, *21*, 1153−1159.

(21) Drobník, J.; Rypáček, F. Soluble synthetic polymers in biological systems. *Adv. Polym. Sci.* **1984**, *57*, 1−50.

(22) Yoshida, M.; Mahato, R. I.; Kawabata, K.; Takakura, Y.; Hashida, M. Disposition characteristics of plasmid DNA in the single-pass rat liver perfusion system. *Pharm. Res*. **1996**, *13*, 599−603.

(23) Fujiwara, M.; Baldeschwieler, J. D.; Grubbs, R. H. Receptor-mediated endocytosis of poly(acrylic acid)-conjugated liposomes by macrophages. *Biochim. Biophys. Acta* **1996**, *1278*, 59−67.

On the basis of the above discussion, the following measures to improve the performance of the delivery system are being proposed. First, a polymer conjugate with molecular weight lower than the renal filtration threshold should be used as such conjugates will eventually be cleared from the body, limiting their deposition to the soft tissues and organs. Their accumulation in the kidneys must, however, be carefully monitored. The lower molecular weight will also lead to a shorter α $T_{1/2}$ and allow a faster access of the delivery system to the bone. Second, the content of D-Asp_8 in the conjugate should be increased. Such improvement will enhance the binding force of the conjugate to bone. Since the binding efficiency depends on the competition between bone binding and renal clearance, a stronger binding force of the conjugate to bone would increase the first pass deposition to bone and increase the overall conjugate deposition to the skeleton. However, the current approach of using a D-Asp_8-containing macromonomer to incorporate the targeting moiety is not very effective. The content of D-Asp_8 in the conjugate is difficult to control, as is evident from Table 1. Polymer-analogous reactions are being investigated to enhance the D-Asp_8 content in the conjugates. As a third potential, a high molecular weight (>45 kDa) but biodegradable polymer carrier may provide a high deposition of the delivery system to the skeleton but also avoid its accumulation in the soft tissues. However, the degradation of the delivery system and its bone-binding process must be well orchestrated to yield an ideal biodistribution profile.

Conclusions

The biodistribution and pharmacokinetic data support the hypothesis that HPMA copolymer−D-Asp_8 conjugates can target to all parts of the skeleton. While increases of the molecular weight of the copolymer may raise the overall conjugate distribution to bone, the selectivity of the delivery system is reduced. Further fine-tuning of the conjugate structure is necessary to optimize its bone-targeting ability. In addition, validation of the delivery system in animal models of osteoporosis and other skeletal diseases is also warranted.

Abbreviations Used

BD, biodistribution; DMSO, dimethyl sulfoxide; HOBt, 1-hydroxybenzotriazole hydrate; HPMA, *N*-(2-hydroxypropyl)methacrylamide; MA-FITC, *N*-methacryloylaminopropyl fluorescein thiourea; MA-Gly-Gly-OH, *N*-methacryloylglycylglycine; MA-Tyr-NH_2, *N*-methacryloyltyrosineamide; M_n, number average molecular weight; M_w, weight average molecular weight; P, tyrosine-labeled HPMA copolymer backbone; P−D-Asp_8, tyrosine-labeled HPMA copolymer−D-Asp_8 conjugate; PDI, polydispersity; PK, pharmacokinetics; PyBOP, benzotriazol-1-yl-oxy-tris-pyrrolidino-phosphonium hexafluorophosphate; SEC, size exclusion chromatography; SPECT, single photon emission computed tomography; SPPS, solid-phase peptide synthesis; $T_{1/2}$, elimination half-life; Vd_{ss}, steady-state volume of distribution.

Acknowledgment. We thank Dr. H. E. Gendelman for valuable discussion and for the permission to use the single photon emission computed tomography equipment. We also thank Dr. Huaiyun Han's technical support in part of the animal experiments. D.W. deeply appreciates the financial support he received as a new faculty member from the College of Pharmacy, UNMC. This work was supported in part by NIH Grant GM069847.

Supporting Information Available: Movies 1 and 2 of tomographic analysis (with SPECT) of Tyr-D-Asp_8's distribution in the skeleton. This material is available free of charge via the Internet at http://pubs.acs.org.

MP0600539